Techniques of evaluation of QCD low-energy physical quantities with running coupling with infrared fixed point

Gorazd Cvetič

Universidad Técnica Federico Santa María (UTFSM), Valparaíso, Chile

in collaboration with
R. Kögerler (Bielefeld), C. Valenzuela (PUC), C. Ayala and C. Contreras (UTFSM), A.V. Kotikov (JINR Dubna)
Universidad Técnica Federico Santa María (UTFSM), Chile

LC2013+ Satellite Meeting, Skiathos, Greece, May 24-25, 2013

Introduction

Perturbative QCD (pQCD) running coupling $a(Q^2)$ ($\equiv \alpha_s(Q^2)/\pi$, where $Q^2 \equiv -q^2$) has unphysical (Landau) singularities at low spacelike momenta $0 < Q^2 \lesssim 1 \ \mathrm{GeV}^2$.

It is expected that the true QCD coupling $\mathcal{A}(Q^2)$ has no such singularities and that it remains smooth and finite at small $|Q^2|$, i.e., that $\beta(\mathcal{A}(Q^2)) \equiv \partial \mathcal{A}(Q^2)/\partial \ln Q^2$ has an infared (IR) fixed point:

$$\beta(\mathcal{A}(0)) = 0, \qquad \mathcal{A}(0) < \infty \ .$$

.

Introduction

This (IR fixed point) behavior is suggested by:

- lattice calculations [Cucchieri and Mendes (PRL, 2008); Bogolubsky et al. (PLB, 2009); Furui (PoS LAT, 2009)];
- calculations based on (Dyson-Schwinger equations (DSE) [Alkofer et al. (PLB, 2005); Aguilar et al. (PRD, 2008, 2009); Binosi and Papavassiliou (Phys. Rept., 2009)];
- light-front holographic mapping AdS/CFT modified by a (positive-sign) dilaton background [Brodsky, de Teramond and Deur, PRD, 2010]

- and is suggested by most of the analytic QCD models, among them:
  1. Analytic Perturbation Theory (APT) of Shirkov, Solovtsov, Solovtsova, Milton et al. (JINR RC, 1996; PRL, 1997; PRD, 1997; PLB, 1997, 1998; EPJC, 2001); also: Karanikas and Stefanis (PLB, 2001).
  2. its extension Fractional APT (FAPT) of Bakulev, Mikhailov and Stefanis (PRD, 2005, 2008; JHEP, 2010);
  3. analytic models with $\mathcal{A}(Q^2)$ very close to $a(Q^2)$ at high $|Q^2| > \Lambda^2$: $\mathcal{A}(Q^2) - a(Q^2) \sim (\Lambda^2/Q^2)^N$ with $N = 3, 4$ or 5 [Webber (JHEP, 1998); [Alekseev (Few Body Syst., 2006); Contreras, G.C., et al. (PRD 2010, 2012)];
  4. Perturbative QCD in confining QCD background, for $N_c \to \infty$ [Simonov (Phys. Atom. Nucl., 2002)].

Introduction

Perturbative QCD (pQCD) can give analytic coupling $a(Q^2)$ in specific schemes with IR fixed point, but with problems in the reproduction of the correct value of $r_\tau \approx 0.20$ [Kögerler, Valenzuela, G.C. (JPG, 2010; PRD, 2010)].
Further, (F)APT also does not reproduce the correct value of r_τ.

The analytic (holomorphic) QCD models are based on the simple requirement that the coupling $\mathcal{A}(Q^2)$ has similar analyticity properties as physical spacelike QCD observables $\mathcal{D}(Q^2)$.
All such couplings, $\mathcal{A}(Q^2)$, differ from the pQCD couplings $a(Q^2)$ at $|Q| \gtrsim 1$ GeV by nonperturbative (NP) terms, typically by some power-suppressed terms $\sim 1/Q^{2N}$ or $1/[Q^{2N} \ln^K(Q^2/\Lambda^2)]$.

IR fixed point scenarios: APT

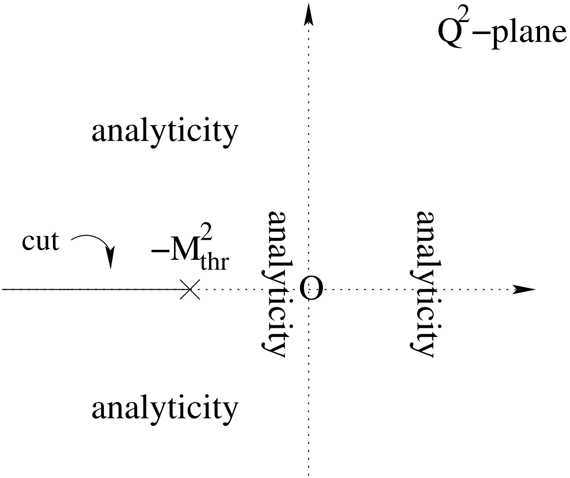

Figure: The typical region of analyticity of a spacelike observable $\mathcal{D}(Q^2)$ in the complex Q^2-plane.

Introduction

Evaluations of physical QCD quantities $\mathcal{D}(Q^2)$ in terms of such $\mathcal{A}(\kappa Q^2)$: usually as (truncated) power series in $\mathcal{A}(\kappa Q^2)$:

$$\mathcal{D}(Q^2) \approx \mathcal{A}(\kappa Q^2) + d_1(\kappa)\mathcal{A}(\kappa Q^2)^2 + d_2(\kappa)\mathcal{A}(\kappa Q^2)^3 + \ldots \tag{1}$$

We argue that such an evaluation approach is not correct:

- The series has increasingly strong κ dependence when the number of terms increases.
- The series has a fast asymptotic divergent behavior due to the renormalon problem.

We show that an alternative series in terms of logarithmic derivatives of $\mathcal{A}(\kappa Q^2)$ should be used instead

$$\widetilde{\mathcal{A}}_n(\mu^2) \propto \partial^{n-1}\mathcal{A}(\mu^2)/\partial(\ln \mu^2)^{n-1} \tag{2}$$

or a $\widetilde{\mathcal{A}}_n$-based resummation (the generalized diagonal Padé method). Timelike low-energy observables are evaluated analogously, using the integral transformation which relates the timelike observable with the corresponding spacelike observable.

IR fixed point scenarios: effective gluon mass

1A) The simplest case of freezing comes from the use of the the one-loop perturbative coupling with the replacement $Q^2 \mapsto Q^2 + m^2$ where $m \sim 1$ GeV is a constant effective gluon mass

$$\mathcal{A}^{(m)}(Q^2) = \frac{1}{\beta_0 \ln\left(\frac{Q^2+m^2}{\Lambda^2}\right)}, \tag{3}$$

where $\beta_0 = (1/4)(11 - 2N_f/3)$. It comes from the use of nonperturbative QCD background [Simonov (Phys.Atom.Nucl., 1995, and arXiv:1011.5386)]. Was used in analysis of the proton structure functions (with $m = m_\rho \approx 0.8$ GeV) [Badelek et al. (Z.Phys.C, 1997)]. See also: Shirkov (arXiv:1208.2103).

This coupling is analytic, in the sense that it has singularities in the complex Q^2-plane on the negative semiaxis only: a pole at $Q^2 = \Lambda^2 - m^2$ (< 0), and a cut at $Q^2 < -m^2$. At $Q^2 \to 0$ the coupling freezes at the positive value $[\beta_0 \ln(m^2/\Lambda^2)]^{-1}$. At large $|Q^2| > \Lambda^2$ it tends to one-loop pQCD coupling and differs from it by $\sim \frac{m^2}{Q^2 \ln^2(Q^2/\Lambda^2)}$.

1B) A range of models with similar running of the coupling is suggested by extensive analyses of the Dyson-Schwinger equations for the gluon and ghost propagators and vertices [Cornwall (PRD, 1982); Aguilar and Papavassiliou (EPJA, 2008)]

$$\mathcal{A}^{(\mathrm{DS},1-\ell.)}(Q^2) = \frac{1}{\beta_0 \ln\left(\frac{Q^2+\rho m(Q^2)^2}{\Lambda^2}\right)} \ , \tag{4}$$

where $\rho \sim 1$ and the running effective gluon mass $m(Q^2)$ is associated with the existence of IR-finite solutions for the gluon propagator $\triangle(Q^2) = 1/(Q^2 + m(Q^2)^2)$: $\triangle(0) < 1/{m_g}^2 < \infty$. This preferred dynamical mass has logarithmic running

$$m(Q^2)^2 \quad = \quad {m_g}^2 \left[\frac{\ln\left(\frac{Q^2+\rho {m_g}^2}{\Lambda^2}\right)}{\ln\left(\frac{\rho {m_g}^2}{\Lambda^2}\right)} \right]^{-1-\gamma_1} \ , \tag{5}$$

where $\gamma_1 \approx 0$, $m_g \approx 0.5$ GeV; $\rho \approx 4$.

IR fixed point scenarios: eff.gl.mass extension to n-loops

1C) At higher $|Q^2|$ ($> \Lambda^2$), when going beyond the one-loop level, the multiplicative renormalizability suggests that the replacement $Q^2 \mapsto (Q^2 + \rho m(Q^2)^2)$ should be made in the perturbative coupling

$$\mathcal{A}^{(\mathrm{DS,n-\ell.})}(Q^2) \approx a^{(n-\ell.)}(Q^2 + \rho m(Q^2)^2) \ , \tag{6}$$

[Luna, dos Santos, Natale (PLB, 2011); when $m = const.$: Shirkov (arXiv:1208.2103); Badalian and Kuzmenko (PRD, 2002)]
The dynamical mass $m(Q^2)$ of the DSE-approaches introduces nonperturbative effects which are felt at $|Q^2| > \Lambda^2$ as

$$\mathcal{A}^{(\mathrm{DS})}(Q^2) - a(Q^2) \sim \frac{m(Q^2)^2}{Q^2 \ln^2(Q^2/\Lambda^2)} \ , \tag{7}$$

and this behaves approximately as $\sim {m_g}^2/(Q^2 \ln^3(Q^2/\Lambda^2))$ when $m(Q^2)$ is logarithmically running.

IR fixed point scenarios: AdS/CFT

2) A model obtained by AdS/CFT correspondence modified by a (positive-sign) dilaton background [Brodsky, de Teramond and A. Deur (PRD, 2010)]

$$\mathcal{A}^{(\mathrm{AdSmod.})}(Q^2) = \mathcal{A}^{(\mathrm{AdS})}(Q^2) g_+(Q^2) + a^{(\mathrm{fit})}(Q^2) g_-(Q^2) \ , \tag{8}$$

where at low $Q < 0.8$ GeV predominates the AdS-part

$$\mathcal{A}^{(\mathrm{AdS})}(Q^2) = \mathcal{A}^{(\mathrm{AdS})}(0) e^{-Q^2/(4k^2)} \ , \tag{9}$$

with $k = 0.54$ GeV; and $\mathcal{A}^{(\mathrm{AdS})}(0) = 1$ is the IR fixed point in g_1 (Bjorken sum rule) effective charge scheme. On the other hand, $a^{(\mathrm{fit})}(Q^2)$ is obtained by fit to the data for $Q > 0.8$ GeV.
$g_{\pm}(Q^2)$ are smeared step functions, e.g., $g_{\pm}(Q^2) = 1/(1 + e^{\pm(Q^2 - Q_0^2)/\tau^2})$ with $Q_0 = 0.8$ GeV and $\tau = k$. At large $|Q^2| > k^2$ the difference between this coupling and the perturbative coupling is very small

$$\mathcal{A}^{(\mathrm{AdSmod.})}(Q^2) - a(Q^2) \sim e^{-Q^2/k^2} \qquad (|Q^2| > k^2) \ . \tag{10}$$

IR fixed point scenarios: APT

3) Analytic Perturbation Theory (APT) coupling constructed by Shirkov and Solovtsov (JINR RC, 1996; PRL, 1997)
See also: Shirkov, Solovtsov, Solovtsova, Milton et al. (PRD, 1997; PLB, 1997, 1998; EPJC, 2001); Karanikas and Stefanis (PLB, 2001).
Construction:
The pQCD coupling $a(Q^2)$ has singularities on the semiaxis $Q^2 < \Lambda_{\rm L}^2$, where the (Landau) cut is $0 < Q^2 < \Lambda_{\rm L}^2$.
Application of the Cauchy theorem to the function $a(Q'^2)/(Q'^2 - Q^2)$ to an appropriate closed contour in the complex Q'^2-plane, leads to the following dispersion relation for $a(Q^2)$

$$a(Q^2) = \frac{1}{\pi} \int_{\sigma=-\Lambda_{\rm L}{}^2}^{\infty} \frac{d\sigma \ \rho^{(\rm pt)}(\sigma)}{(\sigma + Q^2)}, \qquad (11)$$

where $\rho^{(\rm pt)}(\sigma) \equiv {\rm Im} \ a(-\sigma - i\epsilon)$ is the (pQCD) discontinuity functions along the cut.

IR fixed point scenarios: APT

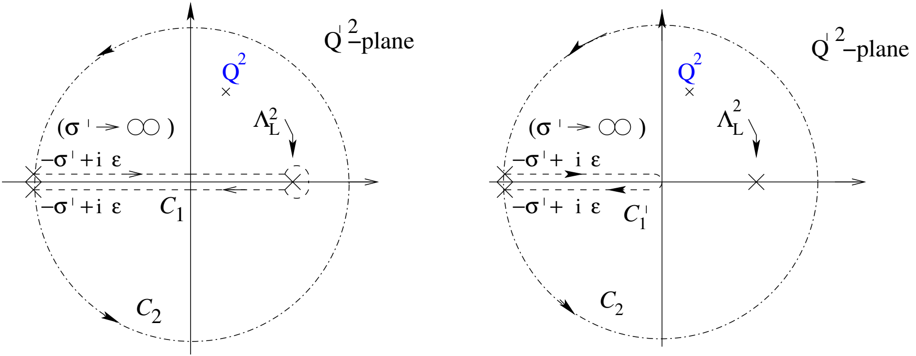

Figure: Left-hand Figure: the integration path for the integrand $a(Q'^2)/(Q'^2 - Q^2)$ leading to the dispersion relation (11) for $a(Q^2)$. Right-hand Figure: the integration path for the same integrand, leading to the dispersion relation (13) for the APT coupling $\mathcal{A}^{(\mathrm{APT})}(Q^2)$.

IR fixed point scenarios: APT

The APT procedure consists in the elimination, in the above integral, of the contributions of the Landau cut $0 < (-\sigma) \leq \Lambda_{\rm L}^2$, leading to the APT analytic analog of a

$$\mathcal{A}^{(\rm APT)}(Q^2) = \frac{1}{\pi} \int_{\sigma=0}^{\infty} \frac{d\sigma \rho^{(\rm pt)}(\sigma)}{(\sigma + Q^2)} \ . \tag{12}$$

The APT analogs of powers a^{ν} (ν a real exponent) are obtained in the same way

$$\mathcal{A}_{\nu}^{(\rm APT)}(Q^2) = \frac{1}{\pi} \int_{\sigma=0}^{\infty} \frac{d\sigma \rho_{\nu}^{(\rm pt)}(\sigma)}{(\sigma + Q^2)} \ , \tag{13}$$

where $\rho_{\nu}^{(\rm pt)}(\sigma) = {\rm Im} a^{\nu}(-\sigma - i\epsilon)$.

IR fixed point scenarios: APT

The underlying pQCD coupling $a(Q^2)$ can run at any n-loop level and can be in any chosen renormalization scheme; the corresponding renormalization group equation (RGE) is

$$\frac{\partial a(\ln Q^2; \beta_2, \ldots)}{\partial \ln Q^2} = - \sum_{j=0}^{n-1} \beta_j \, a^{j+2}(\ln Q^2; \beta_2, \ldots), \qquad (14)$$

where the first two beta coefficients are universal $[\beta_0 = (1/4)(11 - 2N_f/3), \ \beta_1 = (1/16)(102 - 38N_f/3)]$, and the other coefficients β_j ($j \geq 2$) characterize the perturbative renormalization scheme. The APT coupling has IR fixed point: $\mathcal{A}(0) = 1/\beta_0$ $(= 4/9 \approx 0.44$ if $N_f = 3)$. At one-loop level, it is particularly simple:

$$\mathcal{A}^{(\mathrm{APT},1-\ell.)}(Q^2) = \frac{1}{\beta_0} \left[\frac{1}{\ln z} - \frac{1}{(z-1)} \right] \quad (z \equiv Q^2/\Lambda^2) \ . \qquad (15)$$

Explicit expressions for $\mathcal{A}_{\nu}^{(\mathrm{APT})}$ at one-loop level were constructed by Bakulev, Mikhailov and Stefanis (PRD, 2005 and 2008; JHEP, 2010)

$$\left(a_{1\ell}(Q^2)^{\nu}\right)_{\mathrm{an}}^{(\mathrm{APT})} \equiv \mathcal{A}_{\nu}(Q^2)^{(\mathrm{APT},1\ell)} = \frac{1}{\beta_0^{\nu}} \left(\frac{1}{\ln^{\nu}(z)} - \frac{\mathrm{Li}_{-\nu+1}(1/z)}{\Gamma(\nu)} \right) , \tag{16}$$

where $z \equiv Q^2/\Lambda^2$ and $Li_{-\nu+1}(z)$ is the polylogarithm function of order $-\nu+1$; extensions to 2- and 3-loop via expansions [Fractional APT (FAPT)]. For a review of FAPT: Bakulev (Phys. Part. Nucl., 2009).

It turns out that the APT coupling differs from the pQCD coupling by terms $\sim (\Lambda^2/Q^2)$ at large $|Q^2| > \Lambda^2$

$$\mathcal{A}^{(\mathrm{APT})}(Q^2) - a(Q^2) \sim \left(\frac{\Lambda^2}{Q^2} \right)^{1} , \tag{17}$$

which may be appreciable even at high energies.

IR fixed point scenarios: Webber's model

4) An extension of the APT coupling at one-loop, such that the difference between it and the pQCD coupling is $\sim (\Lambda^2/Q^2)^p$, was proposed by Webber (JHEP, 1998)

$$\mathcal{A}^{(\mathrm{W},1-\ell.)}(Q^2) = \frac{1}{\beta_0}\left[\frac{1}{\ln z} + \frac{1}{1-z}\,\frac{z+b}{1+b}\left(\frac{1+c}{z+c}\right)^p\right], \qquad (18)$$

where $z \equiv Q^2/\Lambda^2$ and specific values of parameters were chosen such that the model gives good agreement with a range of data on power corrections: $b = 1/4$, $c = 4$, and $p = 4$. The coupling has IR fixed point, $\mathcal{A}^{(\mathrm{W},1-\ell.)}(0) = 1/(2\beta_0) \approx 0.22$. At large $|Q^2|$, the difference from the pQCD coupling is

$$\mathcal{A}^{(\mathrm{W},1-\ell.)}(Q^2) - a^{(1-\ell.)}(Q^2) \sim \left(\frac{\Lambda^2}{Q^2}\right)^4 . \qquad (19)$$

IR fixed point scenarios: 1δanQCD, 2δanQCD

5) Yet another approach (1δanQCD, 2δanQCD)
by Contreras, Espinosa, Martinez and G.C (PRD, 2010); Ayala, Contreras and G.C. (PRD, 2012).
Based on the general dispersive relation for analytic couplings,

$$\mathcal{A}(Q^2) = \frac{1}{\pi} \int_{\sigma=0}^{\infty} \frac{d\sigma \rho(\sigma)}{(\sigma + Q^2)} \ , \tag{20}$$

where $\rho(\sigma) \equiv \mathrm{Im}\mathcal{A}(-\sigma - i\epsilon)$ is approximated at high momenta $\sigma \geq M_0^2$ by $\rho^{(\mathrm{pt})}(\sigma)$ $[\equiv \mathrm{Im}\ a(-\sigma - i\epsilon)]$, and in the unknown low-momentum regime by one or two deltas:

$$\begin{aligned} \rho(\sigma)^{(1\delta)}(\sigma) &= \pi F_1^2 \delta(\sigma - M_1^2) + \Theta(\sigma - M_0^2)\rho^{(\mathrm{pt})}(\sigma) \ , \qquad (21) \\ \rho(\sigma)^{(2\delta)}(\sigma) &= \pi F_1^2 \delta(\sigma - M_1^2) + \pi F_2^2 \delta(\sigma - M_2^2) + \Theta(\sigma - M_0^2)\rho^{(\mathrm{pt})}(\sigma) \ . \end{aligned}$$

The parameters F_j and M_j of the delta functions and the pQCD-onset scale M_0 were adjusted so that the correct value of the semihadronic tau decay ratio $r_\tau \approx 0.20$ ($V + A$ channel) was reproduced and that the difference from the pQCD coupling at high $|Q^2| > \Lambda^2$ is as suppressed as possible.

IR fixed point scenarios: 1δanQCD, 2δanQCD

$$\mathcal{A}^{(1\delta)}(Q^2) = \frac{F_1^2}{Q^2 + M_1^2} + \frac{1}{\pi} \int_{M_0^2}^{\infty} d\sigma \, \frac{\rho^{(\mathrm{pt})}(\sigma)}{(Q^2+\sigma)} \,, \tag{22a}$$

$$\mathcal{A}^{(2\delta)}(Q^2) = \frac{F_1^2}{Q^2 + M_1^2} + \frac{F_2^2}{Q^2 + M_2^2} + \frac{1}{\pi} \int_{M_0^2}^{\infty} d\sigma \, \frac{\rho^{(\mathrm{pt})}(\sigma)}{(Q^2+\sigma)} \,. \tag{22b}$$

Both models (1δanQCD, 2δanQCD) have IR fixed point, with $\mathcal{A}(0) \leq 1$. The resulting deviations from pQCD at high $|Q^2| > \Lambda^2$ are

$$\mathcal{A}^{(1\delta)}(Q^2) - a(Q^2) \sim \left(\frac{\Lambda^2}{Q^2} \right)^3 \,, \tag{23a}$$

$$\mathcal{A}^{(2\delta)}(Q^2) - a(Q^2) \sim \left(\frac{\Lambda^2}{Q^2} \right)^5 \,. \tag{23b}$$

This suppression is preferred because then OPE can be used and interpreted in the same way as OPE in pQCD: that the higher dimensional nonperturbative terms $\sim 1/(Q^2)^N$ have purely IR origin ($N \leq 2$ in 1δanQCD; $N \leq 4$ in 2δanQCD).

Problems with power series in IR FP frameworks; and solution

For a spacelike physical quantity $\mathcal{D}(Q^2)$ (current correlators, structure function sum rules, etc.) the usual evaluation in pQCD is in power series

$$\mathcal{D}(Q^2)_{\rm pt} \;=\; a(\kappa Q^2) + \sum_{n=1}^{\infty} d_n(\kappa)\; a(\kappa Q^2)^{n+1} \;, \tag{24}$$

where $\mu^2 = \kappa Q^2$ is a renormalization scale ($\kappa \sim 1$). Unless this series is the leading-β_0 resummation or some other partial resummation, the series is known only up to certain order $\sim a^N$ (usually $N=3$ or 4)

$$\mathcal{D}(Q^2;\kappa)_{\rm pt}^{[N]} = a(\kappa Q^2) + \sum_{j=1}^{N-1} d_j(\kappa)\; a(\kappa Q^2)^{j+1} \;. \tag{25}$$

The truncated series has unphysical dependence on the renormalization scale (RS) parameter κ.

Problems with power series in IR FP frameworks; and solution

The more terms are included, the weaker the RS dependence generally

$$\frac{\partial \mathcal{D}_{\rm pt}^{[N]}}{\partial \ln \kappa} = K_N a(\kappa Q^2)^{N+1} + K_{N+1} a(\kappa Q^2)^{N+2} + \cdots \sim a^{N+1} \ , \qquad (26)$$

where $K_N, K_{N+1}, \ldots$ are specific coefficients determined by the original coefficients $d_n(\kappa)$ $(n \leq N-1)$. However, if $a(\kappa Q^2)$ large, RS dependence can be large.

In an IR fixed point framework the coupling $\mathcal{A}(Q^2)$ has NP parts

$$\mathcal{A}(Q^2) - a(Q^2) = T_{\rm NP}(Q^2) \ , \qquad (27)$$

where the term $T_{\rm NP}(Q^2)$ is nonperturbative, i.e., at $|Q^2| > \Lambda^2$ it is a function of $a(Q^2)$, $T_{\rm NP}(Q^2) = F(a(Q^2))$, which is nonanalytic at $a = 0$.

Problems with power series in IR FP frameworks; and solution

For example,

$$T_{\rm NP}(Q^2) \sim \left(\frac{\Lambda^2}{Q^2}\right)^n \approx \exp\left[-\frac{n}{\beta_0 a(Q^2)}\right] , \qquad (28a)$$

$$T_{\rm NP}(Q^2) \sim \exp\left(-\frac{Q^2}{K^2}\right) \sim \exp\left[-\left(\frac{\Lambda^2}{K^2}\right) e^{1/\beta_0 a(Q^2)}\right] . \qquad (28b)$$

If applying now the power series (24) in the IR fixed point scenarios,

$$\mathcal{D}(Q^2;\kappa)^{[N]}_{\rm pt,\mathcal{A}} = \mathcal{A}(\kappa Q^2) + \sum_{j=1}^{N-1} d_j(\kappa)\ \mathcal{A}(\kappa Q^2)^{j+1} , \qquad (29)$$

the inclusion of more terms in this power series tends to make the result increasingly more RS-dependent or the RS dependence is more erratic, due to the NP contributions $\sim T_{\rm NP}(\kappa Q^2)^k \mathcal{A}(\kappa Q^2)^m$ in RS dependence.

Problems with power series in IR FP frameworks; and solution

These aspects are also reflected in the fact that the beta function in all the aforedescribed IR fixed point scenarios, $\beta(\mathcal{A}(Q^2)) \equiv \partial \mathcal{A}(Q^2)/\partial \ln Q^2$, cannot be presented with a power expansion in $\mathcal{A}$, due to NP effects

$$\frac{\partial \mathcal{A}(Q^2)}{\partial \ln Q^2} \neq - \sum_{j \geq 0} \beta_j \mathcal{A}(Q^2)^j \ , \tag{30}$$

in contrast to the perturbative RGE (14).

All this suggests that the analog of the power a^n is not $\mathcal{A}^n$, but rather a nonpower expression $\mathcal{A}_n$. Within the context of APT, this has been noted by the authors of APT, and the construction Eq. (13) really gives $\mathcal{A}_\nu^{(\mathrm{APT})} \neq (A_1{}^{(\mathrm{APT})})^\nu$. However, in general analytic models with finite $\mathcal{A}(0)$, the APT-type of construction of $\mathcal{A}_n$ cannot be made since APT uses only the pQCD couplings a^n (and their discontinuities $\rho_n{}^{(\mathrm{pt})}$).

Problems with power series in IR FP frameworks; and solution

The construction of $\mathcal{A}_n$ (the analog of a^n), is made in such general analytic frameworks with IR fixed point, via a detour by construction of logarithmic derivatives [Valenzuela and G.C. (JPG, 2006; PRD, 2006); for noninteger n: Kotikov and G.C. (JPG, 2012)]. In pQCD these are

$$\widetilde{a}_{n+1}(Q^2) \equiv \frac{(-1)^n}{\beta_0^n n!} \frac{\partial^n a(Q^2)}{\partial (\ln Q^2)^n} \ , \qquad (n = 1, 2, \ldots) \ . \tag{31}$$

We have $\widetilde{a}_{n+1}(Q^2) = a(Q^2)^{n+1} + \mathcal{O}(a^{n+2})$ by RGE. The analytization is a linear operation. Therefore

$$\begin{aligned} a(Q^2)_{\rm an} &= \mathcal{A}(Q^2) \Rightarrow \left(\frac{\partial a(Q^2)}{\partial \ln Q^2} \right)_{\rm an} = \frac{\partial \mathcal{A}(Q^2)}{\partial \ln Q^2} \ \Rightarrow & (32) \\ \widetilde{a}_{n+1}(Q^2)_{\rm an} &= \widetilde{\mathcal{A}}_{n+1}(Q^2), {\rm with:} \ \widetilde{\mathcal{A}}_{n+1}(Q^2) \equiv \frac{(-1)^n}{\beta_0^n n!} \frac{\partial^n \mathcal{A}(Q^2)}{\partial (\ln Q^2)^n} & (33) \end{aligned}$$

where $n = 1, 2, \ldots$.

Problems with power series in IR FP frameworks; and solution

In virtually all IR fixed point (analytic) models we have:
$|\mathcal{A}(Q^2)| > |\widetilde{\mathcal{A}}_2(Q^2)| > |\widetilde{\mathcal{A}}_3(Q^2)| > \cdots$
for any Q^2 (even when $|Q^2|$ is small).
The basic relation (33) then requires reexpression of the power series (24) as a series in logarithmic derivatives $\widetilde{a}_{n+1}(Q^2)$ ("modified" perturbation series, mpt)

$$\mathcal{D}(Q^2)_{\rm mpt} \quad = \quad a(\kappa Q^2) + \sum_{n=1}^{\infty} \widetilde{d}_n(\kappa) \, \widetilde{a}_{n+1}(\kappa Q^2) \ . \tag{34}$$

This leads, after the analytization (33) term-by-term, to the "modified" analytic (man) series

$$\mathcal{D}(Q^2)_{\rm man} \quad = \quad \mathcal{A}(\kappa Q^2) + \sum_{n=1}^{\infty} \widetilde{d}_n(\kappa) \, \widetilde{\mathcal{A}}_{n+1}(\kappa Q^2) \ . \tag{35}$$

This is the basic expression for evaluation of $\mathcal{D}(Q^2)$ in IR FP scenarios.

Problems with power series in IR FP frameworks; and solution

Also the truncated series in log derivatives (mpt)

$$\mathcal{D}(Q^2;\kappa)^{[N]}_{\rm mpt} = a(\kappa Q^2) + \sum_{j=1}^{N-1} \widetilde{d}_j(\kappa)\, \widetilde{a}_{j+1}(\kappa Q^2) \ , \qquad (36)$$

has RS dependence due to truncation, similar to the dependence (26) of the truncated pt series, but even simpler

$$\frac{\partial \mathcal{D}^{[N]}_{\rm mpt}}{\partial \ln \kappa} = -\beta_0 N \widetilde{d}_{N-1}(\kappa) \widetilde{a}_{N+1}(\kappa Q^2) \ . \qquad (37)$$

The truncated modified analytic series is

$$\mathcal{D}(Q^2;\kappa)^{[N]}_{\rm man} \quad = \quad \mathcal{A}(\kappa Q^2) + \sum_{j=1}^{N-1} \widetilde{d}_j(\kappa)\, \widetilde{\mathcal{A}}_{j+1}(\kappa Q^2) \ . \qquad (38)$$

Problems with power series in IR FP frameworks; and solution

The mpt series (34) is just a reorganization of the original perturbation (pt) series (24), so it is also RS-independent. In conjunction with the recurrence relation $\partial \widetilde{a}_n(\kappa Q^2)/\partial \ln \kappa = -\beta_0 n \widetilde{a}_{n+1}(\kappa Q^2)$ which follows from the definition (31), we obtain simple differential relations between $\widetilde{d}_n(\kappa)$:

$$\frac{d}{d \ln \kappa} \widetilde{d}_n(\kappa) = n \beta_0 \widetilde{d}_{n-1}(\kappa) \qquad (n = 1, 2, \ldots) \ . \tag{39}$$

($d_0(\kappa) = \widetilde{d}_0(\kappa) = 1$ by definition). Integrating them, the renormalization scale dependence of the coefficients $\widetilde{d}_n$ is particularly simple

$$\widetilde{d}_n(\kappa) = \widetilde{d}_n(1) + \sum_{k=1}^{n} \left(\begin{array}{c} n \\ k \end{array} \right) \beta_0^k \ \ln^k(\kappa) \widetilde{d}_{n-k}(1) \ . \tag{40}$$

($\kappa \equiv \mu^2/Q^2$; $d_0 = \widetilde{d}_0 = 1$).

Problems with power series in IR FP frameworks; and solution

The coefficients $\widetilde{d}_n(\kappa)$ are obtained from $d_k(\kappa)$'s ($k \leq n$) in the following way. First we express the logarithmic derivatives $\widetilde{a}_{n+1}$ in terms of the powers a^{k+1}, at a given scale Q^2 or $\mu^2 = \kappa Q^2$, using the RGE relations in pQCD for these powers [RGE (14) and its derivatives]

$$\widetilde{a}_2 = a^2 + c_1 a^3 + c_2 a^4 + \cdots \ , \tag{41a}$$

$$\widetilde{a}_3 = a^3 + \frac{5}{2} c_1 a^4 + \cdots \ , \qquad \widetilde{a}_4 = a^4 + \cdots \ , \qquad \text{etc.} \ , \tag{41b}$$

where we use the notation $c_j \equiv \beta_j / \beta_0$.

Problems with power series in IR FP frameworks; and solution

We now invert them

$$a^2 = \widetilde{a}_2 - c_1 \widetilde{a}_3 + \left(\frac{5}{2} {c_1}^2 - c_2 \right) \widetilde{a}_4 + \cdots \ , \qquad (42a)$$

$$a^3 = \widetilde{a}_3 - \frac{5}{2} c_1 \widetilde{a}_4 + \cdots \ , \qquad a^4 = \widetilde{a}_4 + \cdots \ , \qquad \text{etc.} \qquad (42b)$$

Problems with power series in IR FP frameworks; and solution

Replacing these relations into the original perturbation expansion (24) for $\mathcal{D}(Q^2)$, the coefficients $\widetilde{d}_n(\kappa)$ of the reorganized ("modified") expansions (34)-(35) can be read off

$$\widetilde{d}_1(\kappa) = d_1(\kappa) , \qquad \widetilde{d}_2(\kappa) = d_2(\kappa) - c_1 d_1(\kappa) , \tag{43a}$$

$$\widetilde{d}_3(\kappa) = d_3(\kappa) - \frac{5}{2} c_1 d_2(\kappa) + \left(\frac{5}{2} {c_1}^2 - c_2 \right) d_1(\kappa) , \qquad \text{etc.} \tag{43b}$$

Problems with power series in IR FP frameworks; and solution

We can also perform analytization, Eqs. (32)-(33), in relations (42a)-(42b) term-by-term. In this way we obtain the (IR fixed point) analogs of integer powers a^n, $\mathcal{A}_n = (a^n)_{\rm an}$

$$\mathcal{A}_2 \equiv \left(a^2\right)_{\rm an} = \widetilde{\mathcal{A}}_2 - c_1 \widetilde{\mathcal{A}}_3 + \left(\frac{5}{2} {c_1}^2 - c_2 \right) \widetilde{\mathcal{A}}_4 + \cdots \ , \tag{44a}$$

$$\mathcal{A}_3 \equiv \left(a^3\right)_{\rm an} = \widetilde{\mathcal{A}}_3 - \frac{5}{2} c_1 \widetilde{\mathcal{A}}_4 + \cdots \ , \quad \mathcal{A}_4 \equiv \left(a^4\right)_{\rm an} = \widetilde{\mathcal{A}}_4 + \cdots \tag{44b}$$

etc. In general IR FP scenarios, we have

$$\mathcal{A}_n \neq \mathcal{A}^n \ .$$

Problems with power series in IR FP frameworks; and solution

This allows us to reexpress the "modified" analytic series (35) in a form which is in close analogy with the original perturbation series (24)

$$\mathcal{D}(Q^2)_{\rm an} \equiv \mathcal{A}(\kappa Q^2) + \sum_{n=1}^{\infty} d_n(\kappa) \, \mathcal{A}_{n+1}(\kappa Q^2) \ . \qquad (45)$$

This series is κ-independent since it coincides with the series $\mathcal{D}(Q^2)_{\rm man}$ of Eq. (35). The truncated series is

$$\mathcal{D}(Q^2;\kappa)^{[N]}_{\rm an} \equiv \mathcal{A}(\kappa Q^2) + \sum_{n=1}^{N-1} d_n(\kappa) \, \mathcal{A}_{n+1}(\kappa Q^2) \ .$$

$$= \mathcal{D}(Q^2;\kappa)^{[N]}_{\rm man} \equiv \mathcal{A}(\kappa Q^2) + \sum_{j=1}^{N-1} \widetilde{d}_j(\kappa) \, \widetilde{\mathcal{A}}_{j+1}(\kappa Q^2) \ . \qquad (46)$$

[The truncation at $\widetilde{\mathcal{A}}_N$ is assumed in the relations (44).]

Problems with power series in IR FP frameworks; and solution

The quantities $\widetilde{\mathcal{A}}_n$ and $\widetilde{a}_n$ have the same RS dependence relations (just interchanging $\widetilde{\mathcal{A}}_n \leftrightarrow \widetilde{a}_n$). This implies that the structure of the RS-dependence of the truncated mpt series in pQCD, Eq. (37), survives in its analytic form for the truncated (modified) analytic series (38)

$$\frac{\partial \mathcal{D}_{\rm man}^{[N]}}{\partial \ln \kappa} = \frac{\partial \mathcal{D}_{\rm an}^{[N]}}{\partial \ln \kappa} \quad = \quad -\beta_0 N \widetilde{d}_{N-1}(\kappa) \widetilde{\mathcal{A}}_{N+1}(\kappa Q^2) \ , \qquad (47)$$

These relations, in conjunction with the mentioned hierarchy $|\mathcal{A}(Q^2)| > |\widetilde{\mathcal{A}}_2(Q^2)| > \ldots$, at all Q^2 (not just high $|Q^2|$), suggest: the truncated analytic series $\mathcal{D}_{\rm man}^{[N]}(Q^2;\kappa)$ [Eqs. (38) and (46)] have in general weaker, or less erratic RS dependence (than the power series) when the number of terms increases. This is true even when $|Q^2|$ is low, in contrast to the case of perturbative truncated series $\mathcal{D}(Q^2;\kappa)_{\rm pt}^{[N]}$ and $\mathcal{D}(Q^2;\kappa)_{\rm mpt}^{[N]}$. The construction is applicable in any analytic QCD (even without IR FP).

Problems with power series in IR FP frameworks; and solution

The above considerations can be extended to the case of dependence on the scheme parameters $c_j = \beta_j/\beta_0$ ($j = 2, 3, \ldots$).
The basic pQCD relations are the "scheme RGEs" [Stevenson (PRD, 1981)]

$$\frac{\partial a}{\partial c_2} = a^3 + \mathcal{O}(a^5) \Rightarrow \frac{\partial a^2}{\partial c_2} = 2a^4 + \cdots \ , \tag{48a}$$

$$\frac{\partial a}{\partial c_3} = \frac{1}{2} a^4 + \cdots \ . \tag{48b}$$

For the IR fixed point scenarios (or any analytic model of $\mathcal{A}$), we can define the same scheme dependence, under the correspondence $a^n \leftrightarrow \mathcal{A}_n$

$$\frac{\partial \mathcal{A}}{\partial c_2} = \mathcal{A}_3 + \mathcal{O}(\mathcal{A}_5) \Rightarrow \frac{\partial \mathcal{A}_2}{\partial c_2} = 2\mathcal{A}_4 + \cdots \ , \tag{49a}$$

$$\frac{\partial \mathcal{A}}{\partial c_3} = \frac{1}{2} \mathcal{A}_4 + \cdots \ . \tag{49b}$$

Problems with power series in IR FP frameworks; and solution

These differential equations can be rewritten in terms of $\widetilde{\mathcal{A}}_n$'s using the relations (44). All the scheme dependence relations in pQCD now carry over to IR fixed point scenarios, under the correspondence $a^n \leftrightarrow \mathcal{A}_n$ (or equivalently $\widetilde{a}_n \leftrightarrow \widetilde{\mathcal{A}}_n$)

$$\frac{\partial \mathcal{D}_{\rm pt}^{[N]}}{\partial c_j} = K_N^{(j)} a^{N+1}(\kappa Q^2) + K_{N+1}^{(j)} a^{N+2}(\kappa Q^2) + \cdots \ , \tag{50a}$$

$$\Rightarrow \frac{\partial \mathcal{D}_{\rm an}^{[N]}}{\partial c_j} = K_N^{(j)} \mathcal{A}_{N+1}(\kappa Q^2) + K_{N+1}^{(j)} \mathcal{A}_{N+2}(\kappa Q^2) + \cdots \ , \tag{50b}$$

and analogously for $\mathcal{D}_{\rm man}^{[N]}$.

Problems with power series in IR FP frameworks; and solution

Until now, we took n integer in the construction of $\widetilde{\mathcal{A}}_n$ and $\mathcal{A}_n$. For noninteger $n = \nu$ these quantities were obtained by Kotikov and G.C. (JPG, 2012), via an analytic continuation of the general formulas in $n \mapsto \nu$. For this, we first obtain a dispersion relation for the logarithmic derivatives $\widetilde{\mathcal{A}}_{n+1}(Q^2)$ of Eq. (33), by applying the logarithmic derivatives on the dispersion relation (20) for $\mathcal{A}(Q^2)$

$$\widetilde{\mathcal{A}}_{n+1}(Q^2) = \frac{1}{\pi} \frac{(-1)}{\beta_0^n \Gamma(n+1)} \int_0^\infty \frac{d\sigma}{\sigma} \rho(\sigma) \mathrm{Li}_{-n}(-\sigma/Q^2) \ , \qquad (51)$$

where we recall that $\rho(\sigma) \equiv \mathrm{Im}\mathcal{A}(-\sigma - i\epsilon)$. Then $n \mapsto \nu$ gives

$$\widetilde{\mathcal{A}}_{\nu+1}(Q^2) = \frac{1}{\pi} \frac{(-1)}{\beta_0^\nu \Gamma(\nu+1)} \int_0^\infty \frac{d\sigma}{\sigma} \rho(\sigma) \mathrm{Li}_{-\nu}\left(-\frac{\sigma}{Q^2}\right) \quad (-1 < \nu) \ , \qquad (52)$$

where ν can now be noninteger.

Problems with power series in IR FP frameworks; and solution

The couplings $\mathcal{A}_\nu$ (analytic analogs of powers a^ν), are then obtained as a linear combination of the quantities $\widetilde{\mathcal{A}}_{\nu+m}$ ($m = 0, 1, 2, \ldots$), via a generalization of the relations (44) to any integer n and then replacing $n \mapsto \nu$

$$\mathcal{A}_\nu \equiv \widetilde{\mathcal{A}}_\nu + \sum_{m \geq 1} \widetilde{k}_m(\nu) \widetilde{\mathcal{A}}_{\nu+m} \quad (\nu > 0) \; . \tag{53}$$

The coefficients $\widetilde{k}_m(\nu)$ involve Gamma functions $\Gamma(x)$ and their derivatives (up to m derivatives) at the values $x = 1, \nu + 1, \nu + 2, \ldots, \nu + m$, cf. App. A of Kotikov and G.C. (JPG, 2012).

It turns out that in the (fractional) APT model of (of Shirkov, Solovtsov et al.; and of Bakulev, Mikhailov and Stefanis), the (fractional) power analogs $\mathcal{A}_\nu^{(\mathrm{APT})}$, Eq. (13), constructed entirely from the discontinuities of the pQCD coupling a^ν, coincide with the result of the general approach described here, for the corresponding special (APT) case: $\rho(\sigma) = \rho^{(\mathrm{pt})}(\sigma)$, i.e., when $\mathrm{Im}\mathcal{A}(-\sigma - i\epsilon) = \mathrm{Im}a(-\sigma - i\epsilon)$.

Numerical evidence (Adler function): RScl dependence of truncated series

Renormalization scale dependence of truncated series

We illustrate numerically the arguments of the previous Section, for the various truncated series within various IR fixed point frameworks. We use for the spacelike observable $\mathcal{D}(Q^2)$ the massless effective charge of the Adler function

$$d_{\rm Adl}(Q^2) \equiv -(2\pi^2) \frac{d\Pi(Q^2)}{d \ln Q^2} - 1 \ , \tag{54}$$

whose pQCD power expansion (pt) is

$$d_{\rm Adl}(Q^2)_{\rm pt} = a(Q^2) + d_1 a(Q^2)^2 + \cdots \ , \tag{55}$$

and where $\Pi(Q^2) = \Pi_V(Q^2) + \Pi_A(Q^2)$ ($= 2\Pi_V(Q^2)$, in the massless case) is the correlator of the nonstrange charged hadronic currents

$$\Pi^V_{\mu\nu}(q) = i \int d^4x \ \exp(iq \cdot x) \langle T V_\mu(x) V_\nu(0)^\dagger \rangle = (q_\mu q_\nu - g_{\mu\nu} q^2) \Pi_V(Q^2),$$

where: $V_\mu = \overline{u} \gamma_\mu d$.

Numerical evidence (Adler function): RScl dependence of truncated series

The leading-β_0 (LB) part of this spacelike quantity is known

$$
\begin{aligned}
d_{\rm Adl}^{\rm (LB)}(Q^2)_{\rm (m)pt} &= \int_0^\infty \frac{dt}{t} \, F_{\mathcal{D}}(t) a(t Q^2 e^{\overline{\mathcal{C}}}) && \text{(56a)} \\
&= a(Q^2) + \widetilde{d}_1^{\rm (LB)} \widetilde{a}_2(Q^2) + \cdots + \widetilde{d}_n^{\rm (LB)} \widetilde{a}_{n+1}(Q^2) + \cdots && \text{(56b)} \\
&= a(Q^2) + d_1^{\rm (LB)} a(Q^2)^2 + \cdots d_n^{\rm (LB)} a(Q^2)^{n+1} + \cdots \ , && \text{(56c)}
\end{aligned}
$$

where $F_{\mathcal{D}}(t) \equiv w_{\mathcal{D}}(t) t$ is the characteristic function of the Adler function obtained by Neubert (PRD, 1995) on the basis of the LB expansion coefficients $\widetilde{d}_n^{\rm (LB)} \equiv \widetilde{d}_{n,n} \beta_0^n$. The latter were obtained from the LB Borel transform [Beneke (PLB, 1993; NPB, 1993); Broadhurst (ZPC, 1993)] in the "V" scale convention ($\overline{\mathcal{C}} = 0$). Here $\widetilde{d}_n^{\rm (LB)}$'s are changed to the $\overline{\rm MS}$ scale convention ($\overline{\mathcal{C}} = -5/3$). We note that in general $\widetilde{d}_n^{\rm (LB)} \neq d_n^{\rm (LB)}$ (only at one-loop level $d_n^{\rm (LB)} = \widetilde{d}_n^{\rm (LB)}$).

Numerical evidence (Adler function): RScl dependence of truncated series

The coefficients $\widetilde{d}_n^{(\mathrm{LB})}$ can be represented as

$$\widetilde{d}_n^{(\mathrm{LB})} = (-\beta_0)^n \int_{t=0}^{\infty} d(\ln t) \ln^n \left(t e^{\overline{\mathcal{C}}} \right) F_{\mathcal{D}}(t) \ . \tag{57}$$

We perform the evaluations in the $c_2 = c_3 = \ldots = 0$ renormalization scheme, where the pQCD running coupling $a(\kappa Q^2)$ is expressed with the Lambert function $W_{\mp 1}(z)$

$$a(\kappa Q^2) = -\frac{1}{c_1} \frac{1}{[1 + W_{\mp 1}(z)]} \ . \tag{58}$$

Here, $Q^2 = |Q^2| \exp(i\phi)$; W_{-1} and W_{+1} are the branches of the Lambert function for $0 \leq \phi < +\pi$ and $-\pi < \phi < 0$, respectively, and z is defined as

$$z = -\frac{1}{c_1 e} \left(\frac{\kappa |Q^2|}{\Lambda_{\mathrm{Lam.}}^2} \right)^{-\beta_0/c_1} \exp\left(-i\beta_0\phi/c_1\right) \ , \tag{59}$$

where $\Lambda_{\mathrm{Lam.}}$ is the Lambert QCD scale.

Numerical evidence (Adler function): RScl dependence of truncated series

We vary the renormalization scheme $\mu^2 = \kappa Q^2$, and perform evaluations in various IR fixed point frameworks, with $N_f = 3$:

- The case of constant effective gluon mass m (Simonov; Badelek et al.): Eq. (6), applying it to the coupling a of Eq. (58)
$$\mathcal{A}^{(m)}(\mu^2) = a(\mu^2 + m^2) \ , \tag{60}$$
where we take $m = 0.8$ GeV and $\Lambda_{\rm Lam.} = 0.487$ GeV, giving at $\mu^2 = m_\tau^2$ the value $\mathcal{A}(m_\tau^2) = 0.293/\pi$.
- The DSE-motivated case of a logarithmically running effective gluon mass $m(\mu^2)$ [Cornwall; Aguilar and Papavassiliou] Eq. (5) in conjunction with Eq. (6) applied to the coupling a
$$\mathcal{A}^{(m_{\rm gl})}(\mu^2) = a(\mu^2 + m(\mu^2)^2) \ , \tag{61}$$
where we choose the parameter values $\rho = 4$, $\gamma_1 = 1/11$ (Cornwall, 1982), $m_g = 0.4$ GeV, and $\Lambda = \Lambda_{\rm Lam.} \times 0.72882 = 0.355$ GeV. This gives $\mathcal{A}(m_\tau^2) = 0.300/\pi$.

Numerical evidence (Adler function): RScl dependence of truncated series

- The (fractional) analytic perturbation theory (F)APT case (of Shirkov, Solovtsov el al.; and of Bakulev, Mikhailov and Stefanis), Eq. (13). The APT scale is fixed at $\Lambda_{\rm Lam.}(\rm APT) = 0.572$ GeV, and $N_f = 3$, giving the value ${\mathcal{A}_1}^{(\rm APT)}(m_\tau^2) = 0.295/\pi$.
- The analytic QCD case with one delta function in the low-σ region for the analyticity function (Contreras, Espinosa, Martinez and G.C.), Eqs. (22a) and (23a). This model is numerically very close to pQCD coupling (58), with the exception of the regime $|\mu^2| < 1 \ {\rm GeV}^2$. The input values of the model are those used in Kotikov and G.C. (JPG, 2012) (among them: $\Lambda_{\rm Lam.} = 0.487$ GeV) and give the value ${\mathcal{A}_1}^{(1\delta)}(m_\tau^2) = 0.306/\pi$.

Numerical evidence (Adler function): RScl dependence of truncated series

Furthermore, the first three full (i.e., LB+beyondLB) coefficients d_1, d_2 and d_3 of the Adler function are now exactly known [Baikov, Chetyrkin and Kühn (PRL, 2008)]

$$d_{\rm Adl}(Q^2)^{[4]}_{\rm pt} = a(Q^2) + d_1 a(Q^2)^2 + d_2 a(Q^2)^3 + d_3 a(Q^2)^4 \ . \qquad (62)$$

So the full Adler function can be evaluated at order 4 (TS[4]) or lower, in any scheme and at any scale $\mu^2 = \kappa Q^2$, for example in pQCD and in the aforementioned four IR fixed point frameworks.
The results of the LB Adler function, truncated at order 4 and 6, as power series and as series in log derivatives, for $Q^2 = 1 \ {\rm GeV}^2$, are presented as functions of the squared (spacelike) renormalizations scale $\mu^2 = \kappa Q^2$ in Fig. 3 for the pQCD case, and in Figs. 4 and 5 for the four considered IR fixed point frameworks. Truncations are made at $\sim \mathcal{A}^4$ and $\sim \mathcal{A}^6$ for power series, and at $\widetilde{\mathcal{A}}_4$ and $\widetilde{\mathcal{A}}_6$ for the series in log derivatives.

Numerical evidence (LB Adler function): RScl dependence of truncated series

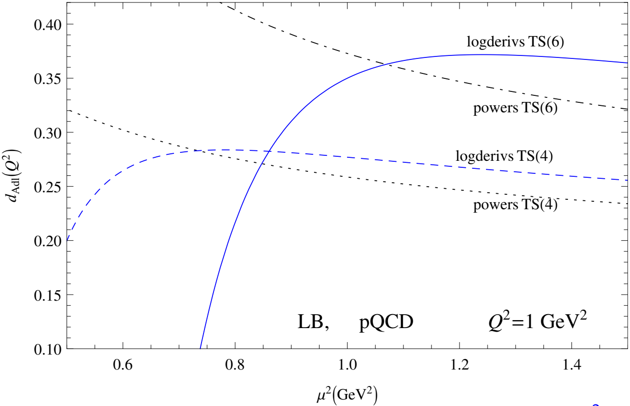

Figure: 3: The effective charge of the massless Adler function $d_{\rm Adl}(Q^2)$, at leading-β_0 (LB), for $Q^2 = 1\ {\rm GeV}^2$, as a function of the (squared) spacelike renormalization scale μ^2, in the case of pQCD [Eq. (58)]. The results of the truncated power series, and of the truncated series in log derivatives, are given. The truncations are made at $\sim a^4$ ($\widetilde{a}_4$) and $\sim a^6$ ($\widetilde{a}_6$).

Numerical evidence (LB Adler function): RScl dependence of truncated series

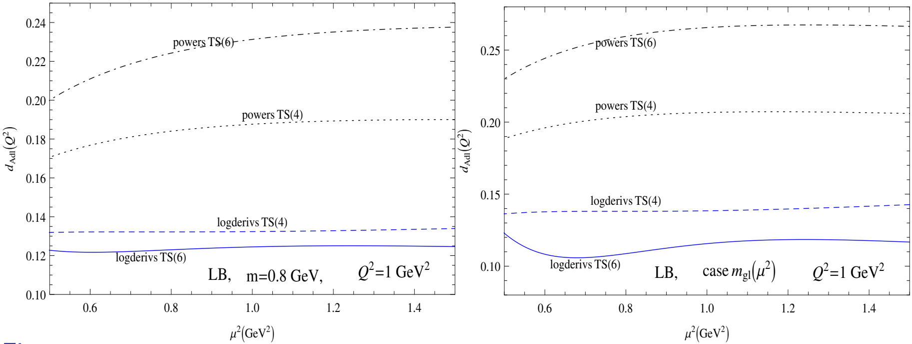

Figure: 4: The same as in Fig. 3, but for the s of the truncated power series, and of the truncated IR fixed point frameworks: (a) with the constant effective gluon mass $m = 0.8$ GeV (the left-hand Figure); (b) with the logarithmically running effective gluon mass (the right-hand Figure). The truncations are made at $\sim \mathcal{A}^4$ ($\widetilde{\mathcal{A}}_4$) and $\sim \mathcal{A}^6$ ($\widetilde{\mathcal{A}}_6$).

Numerical evidence (LB Adler function): RScl dependence of truncated series

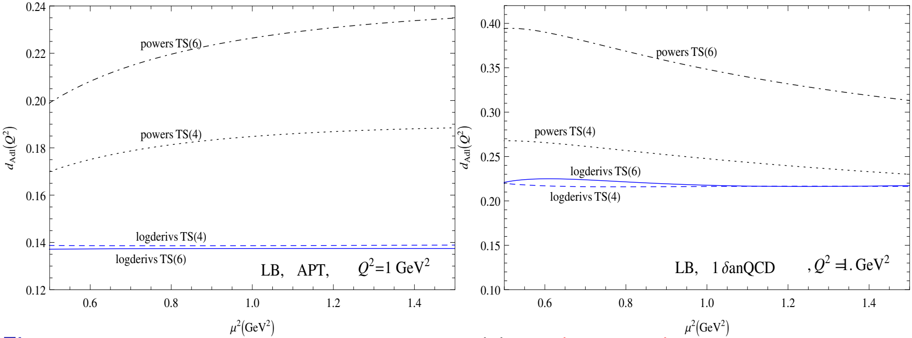

Figure: 5: The same as in Fig. 3, but for the (a) the (fractional) analytic perturbation theory (F)APT (the left-hand Figure); and (b) the analytic model 1δanQCD which has, in the discontinuity function of $\mathcal{A}(Q^2)$, one delta function in the low-σ regime (the right-hand Figure). The truncations are made at $\sim \mathcal{A}^4$ ($\widetilde{\mathcal{A}}_4$) and $\sim \mathcal{A}^6$ ($\widetilde{\mathcal{A}}_6$).

Numerical evidence (LB+bLB Adler function): RScl dependence of truncated series

Furthermore, the analogous results based on the truncated series (62) with s of the truncated power series, and of the truncated full (LB+bLB) coefficients, are given for pQCD in Fig. 6, and for the four considered IR fixed point cases in Figs. 7 and 8. Truncations are made at $\sim \mathcal{A}^3$ ($\widetilde{\mathcal{A}}_3$) and $\sim \mathcal{A}^4$ ($\widetilde{\mathcal{A}}_4$).

Numerical evidence (LB+bLB Adler function): RScl dependence of truncated series

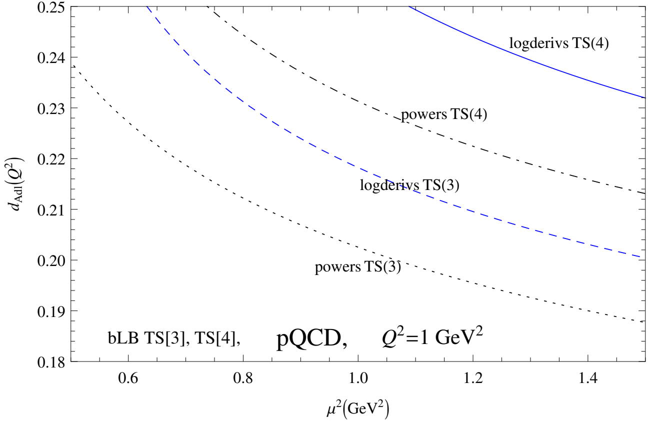

Figure: 6: The same as in Fig. 3, in pQCD, but for the truncated series with the full (LB+beyondLB) coefficients, cf. Eq. (62). The truncations are made at $\sim a^3$ ($\widetilde{a}_3$) and $\sim a^4$ ($\widetilde{a}_4$).

Numerical evidence (LB+bLB Adler function): RScl dependence of truncated series

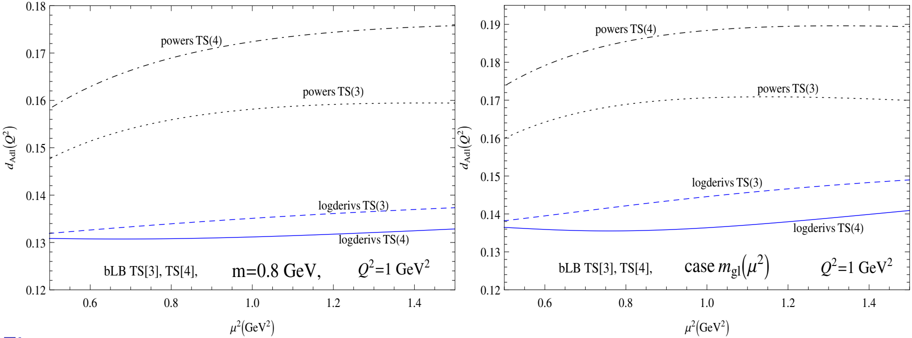

Figure: 7: The same as in Fig. 4, for IR fixed point frameworks with effective gluon mass, but for the truncated series with the full (LB+beyondLB) coefficients, cf. Eq. (62). The truncations are made at $\sim \mathcal{A}^3$ ($\widetilde{\mathcal{A}}_3$) and $\sim \mathcal{A}^4$ ($\widetilde{\mathcal{A}}_4$).

Numerical evidence (LB+bLB Adler function): RScl dependence of truncated series

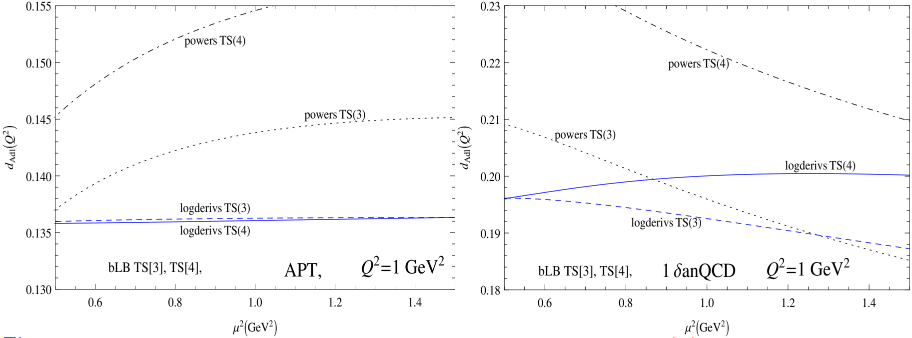

Figure: 8: The same as in Fig. 5, for IR fixed point frameworks (F)APT and 1δanQCD, but for the truncated series with the full (LB+beyondLB) coefficients, cf. Eq. (62). The truncations are made at $\sim \mathcal{A}^3$ ($\widetilde{\mathcal{A}}_3$) and $\sim \mathcal{A}^4$ ($\widetilde{\mathcal{A}}_4$).

Numerical evidence (Adler function): RScl dependence of truncated series

These figures show how the arguments of the previous Section manifest themselves in practice. In the IR fixed point frameworks, the truncated power expansions have increasingly strong renormalization scale dependence (when the number of terms increases), due to the wrong incorporation of the NP contributions at higher orders there. This effect is stronger when Q^2 values are lower. On the other hand, the truncated expansions in log derivatives, in the IR fixed point frameworks, have weaker scale dependence, and this dependence gets in general weaker when the number of terms in the truncated series increases. Furthermore, these figures indicate that the power series has divergent behavior already at relatively low orders, in contrast to the series in log derivatives.
On the other hand, in pure pQCD scenario, the two types of truncated series give comparable results, not clear which one is better, as demonstrated also in: Loewe, Martinez, Valenzuela and G.C. (PRD, 2010).

Numerical evidence (Adler function): convergence properties

Convergence properties

We present, for $\mathcal{D}(Q^2) = d_{\rm Adl}(Q^2)$, the convergence properties: (a) of truncated series in powers; (b) in log derivatives; (c) of a resummed version of the latter based on generalized diagonal Padé's (dPA). This method was introduced by G.C. (NPB, 1998; PRD, 1998) in the context of pQCD, later applied to analytic QCD frameworks in [Kögerler and G.C. (PRD, 2011); Villavicencio and G.C. (PRD, 2012)]. It has the form

$$\mathcal{G}_{\mathcal{D}}^{[M/M]}(Q^2) = \sum_{j=1}^{M} \widetilde{\alpha}_j \, \mathcal{A}(\kappa_j Q^2) \ , \qquad (63)$$

where κ_j and $\widetilde{\alpha}_j$ ($\widetilde{\alpha}_1 + \ldots + \widetilde{\alpha}_M = 1$) are determined from the known truncated series of the observable $\mathcal{D}(Q^2)$ up to $\widetilde{a}_{2M}$ ($\sim a^{2M}$)

$$\mathcal{D}(Q^2;\mu^2)^{[2M]}_{\rm mpt} = a(\mu^2) + \sum_{j=1}^{2M-1} \widetilde{d}_j(\mu^2/Q^2) \, \widetilde{a}_{j+1}(\mu^2) \ . \qquad (64)$$

Numerical evidence (Adler function): convergence properties

κ_j and $\widetilde{\alpha}_j$ are obtained by regarding the log derivatives series (64) as formally a series in powers of one-loop coupling ($\widetilde{a}_{j+1} \mapsto {a_{1\ell}}^{j+1}$)

$$\widetilde{\mathcal{D}}(Q^2;\mu^2)_{\rm pt}^{[2M]} = a_{1\ell}(\mu^2) + \sum_{j=1}^{2M-1} \widetilde{d}_j(\mu^2/Q^2)\, a_{1\ell}(\mu^2)^{j+1} \ , \qquad (65)$$

and constructing for it the diagonal Padé (dPA) $[M/M]$ which is then decomposed in a linear combination of simple fractions

$$[M/M]_{\widetilde{\mathcal{D}}}(a_{1\ell}(\mu^2)) = \sum_{j=1}^{M} \widetilde{\alpha}_j \frac{x}{1+\widetilde{u}_j x}\bigg|_{x=a_{1\ell}(\mu^2)} \ . \qquad (66)$$

$[M/M]_{\widetilde{\mathcal{D}}}$ is by definition a ratio of two polynomials in $a_{1\ell}(\mu^2)$ of order M each, and whose coefficients are determined by the condition: $[M/M]_{\widetilde{\mathcal{D}}} - \widetilde{\mathcal{D}}(Q^2;\mu^2)_{\rm pt}^{[2M]} \sim {a_{1\ell}}^{2M+1}$.

Numerical evidence (Adler function): convergence properties

We have $x/(1+\widetilde{u}_j x) = a_{1\ell}(\kappa_j Q^2)$ (with: $x = a_{1\ell}(\mu^2)$), i.e.

$$[M/M]_{\widetilde{\mathcal{D}}}(a_{1\ell}(\mu^2)) = \sum_{j=1}^{M} \widetilde{\alpha}_j \, a_{1\ell}(\kappa_j Q^2) \ , \quad \text{where } \kappa_j Q^2 = \mu^2 \exp(\widetilde{u}_j/\beta_0) \ . \tag{67}$$

This procedure gives $\widetilde{\alpha}_j$ and κ_j; they are exactly-independent of the chosen renormalization scale μ^2, and $\mathcal{G}_{\mathcal{D}}^{[M/M]}(Q^2)$, Eq. (63), fulfills the basic order $N = 2M$ approximant requirement

$$\mathcal{D}(Q^2) - \mathcal{G}_{\mathcal{D}}^{[M/M]}(Q^2) = \mathcal{O}(\widetilde{\mathcal{A}}_{2M+1}) = \mathcal{O}(\mathcal{A}_{2M+1}) \ . \tag{68}$$

As shown in [Kögerler and G.C. (PRD, 2011); Villavicencio and G.C. (PRD, 2012)], these approximants work very well in the analytic QCD frameworks.

Numerical evidence (LB Adler function): convergence properties

Using the LB Adler function, Eqs. (56) and (57), as a test case, at $Q^2 = 1 \ \mathrm{GeV}^2$, we present in Figs. 9 the results of the evaluation of this "quasi-observable" as a function of the truncation order N in the case of pQCD coupling a, Eq. (58), as: truncated power series, truncated series in logarithmic derivatives, and the generalized dPA's Eq. (63) (in that case: $N = 2M = 2, 4, \ldots$).

We can see that the power series and the series in log derivatives increase with increasing N above the exact value[1], while the generalized dPA oscillates uncontrollably around it.

[1] The "exact" value is here taken as the Principal Value of the integral (56a) which has ambiguity due to Landau singularities of pQCD coupling. No such ambiguity problems appear in the other considered cases, because they have IR fixed point.

Numerical evidence (LB Adler function): convergence properties

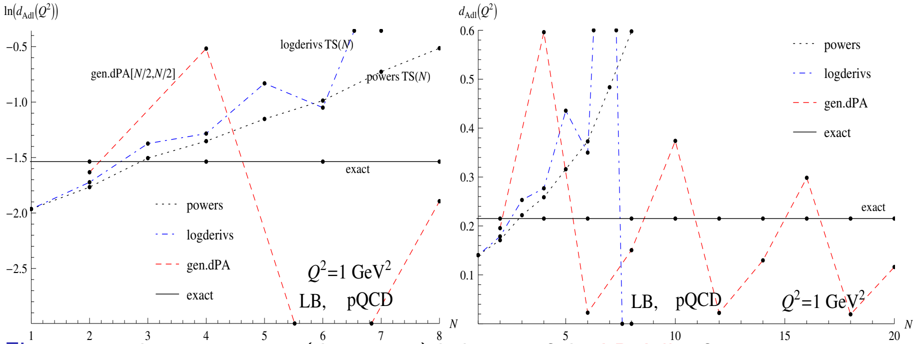

Figure: 9: The convergence (divergence) behavior of the LB Adler function at $Q^2 = 1\ \mathrm{GeV}^2$, as a function of the truncation order N, in pQCD. The left-hand Figure is for a larger interval of values of the LB Adler function - the vertical axis represents $\ln d_{\rm Adl}^{(\rm LB)}(Q^2))$. The right-hand Figure is for a narrower interval of values $d_{\rm Adl}^{(\rm LB)}(Q^2)$, and for a larger N-interval.

Numerical evidence (LB Adler function): convergence properties

In Figs. 10 and 11 we present the corresponding results for the gluon effective mass case: $m = 0.8$ GeV case of Eq. (60), and the running mass case of Eq. (61), respectively.
Finally, In Figs. 12 and 13 we present the results for the (F)APT model of Eq. (13), and 1δanQCD model of Eqs. (22a) and (23a), respectively.

Numerical evidence (for: LB Adler function): convergence properties

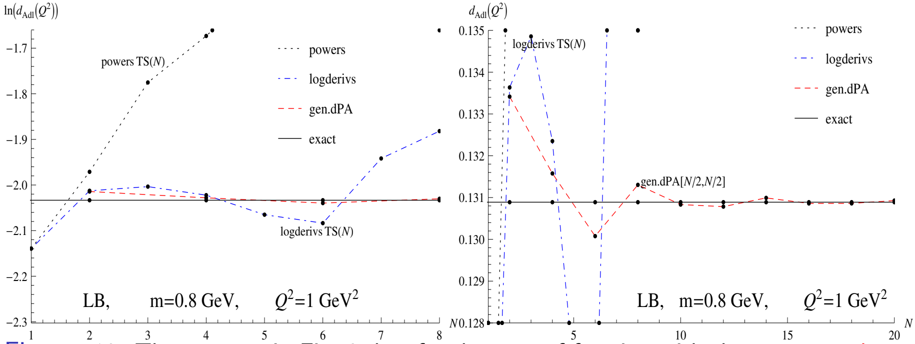

Figure: 10: The same as in Fig. 9, but for the case of freezing with the constant gluon effective mass $m = 0.8$ GeV.

Numerical evidence (LB Adler function): convergence properties

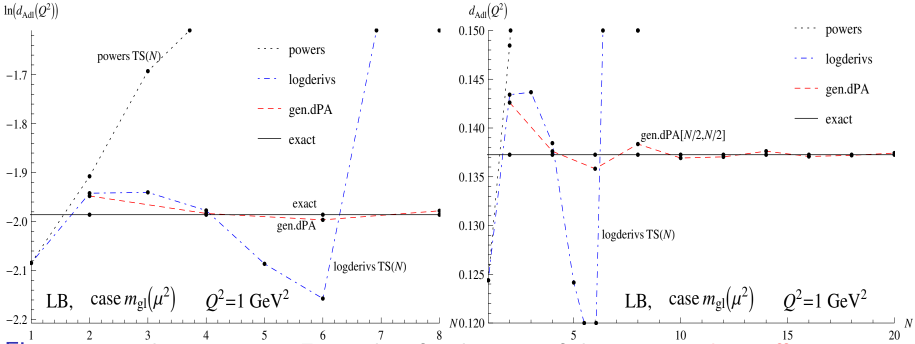

Figure: 11: The same as in Fig. 9, but for the case of the running gluon effective mass $m_{gl}(Q^2)$.

Numerical evidence (LB Adler function): convergence properties

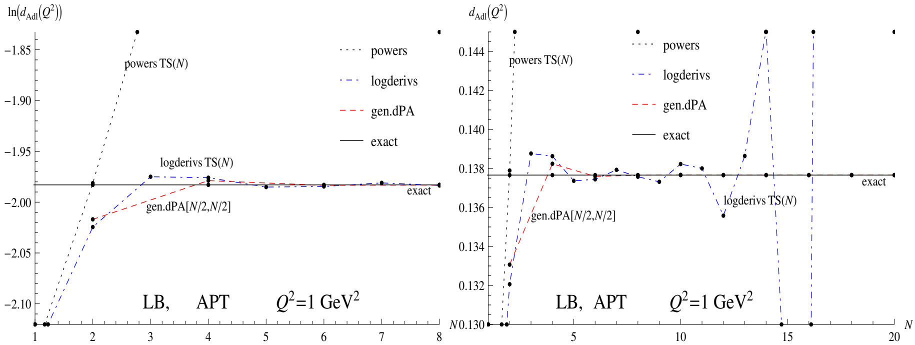

Figure: 12: The same as in Fig. 9, but for the case of (F)APT model.

Numerical evidence (for: LB Adler function): convergence properties

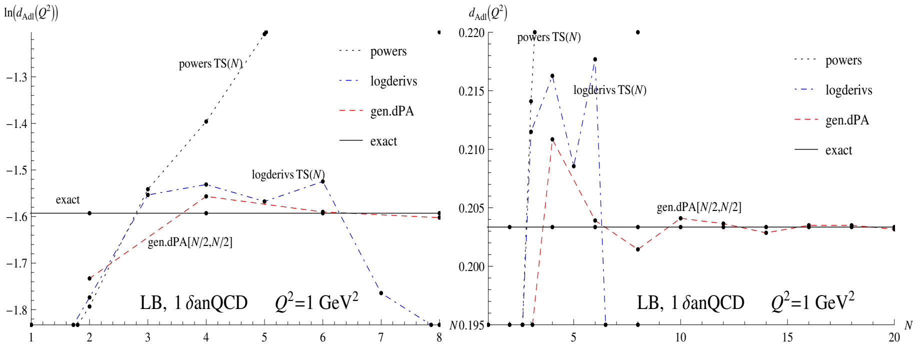

Figure: 13: The same as in Fig. 9, but for the case of 1δ analytic QCD model.

Numerical evidence (LB Adler function): convergence properties

We can see that, in any framework with IR fixed point, the series in log derivatives has a clearly better convergence than the power series.
The power series (although with $\mathcal{A}(Q^2) < 1$) is badly divergent.
Both series (in powers and in log derivatives) have renormalon growth of the coefficients: $d_n \sim \widetilde{d}_n \sim n!$ when n large. And at any Q^2, the hierarchies hold:
a) $\mathcal{A}(Q^2) > \mathcal{A}(Q^2)^2 > \mathcal{A}(Q^2)^3 > \ldots$
b) $\mathcal{A}(Q^2) > |\widetilde{\mathcal{A}}_2(Q^2)| > |\widetilde{\mathcal{A}}_3(Q^2)| > \ldots$.
Nonetheless, the log derivatives $\widetilde{\mathcal{A}}_n(Q^2)$ have alternating signs at large n, which numerically explains why such a series has better convergence than the power series.
The results of the Figures further indicate that the generalized dPA method works very well in all the frameworks with IR fixed point, there appears no divergent behavior.

Numerical evidence (LB+bLB Adler function): convergence properties

Finally, in Fig. 14 we present analogous results as in Fig. 9, for pQCD, but this time with the known full (LB+beyondLB) coefficients d_n ($\widetilde{d}_n$), cf. Eq. (62). Since only up to d_4 ($\widetilde{d}_4$) coefficients are known exactly, the results are shown only up to the order $N = 4$.

In Figs. 15 and 16 the analogous results for the four considered IR fixed point frameworks are shown.

Numerical evidence (LB+bLB Adler function): convergence properties

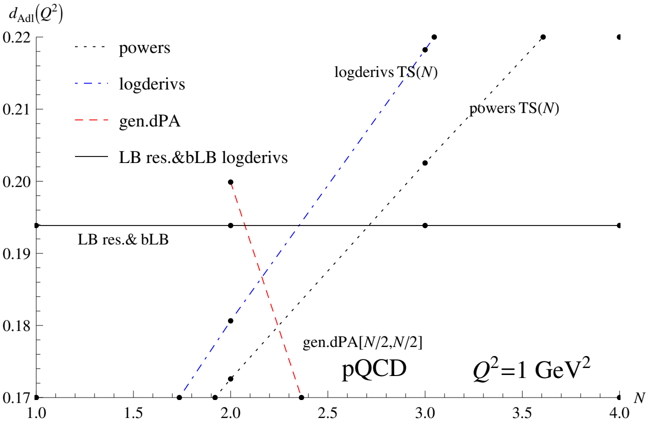

Figure: 14: Analogous results as those of Fig. 9, in pQCD, but for the truncated series based on the full (LB+beyondLB) coefficients, cf. Eq. (62)

Numerical evidence (LB+bLB Adler function): convergence properties

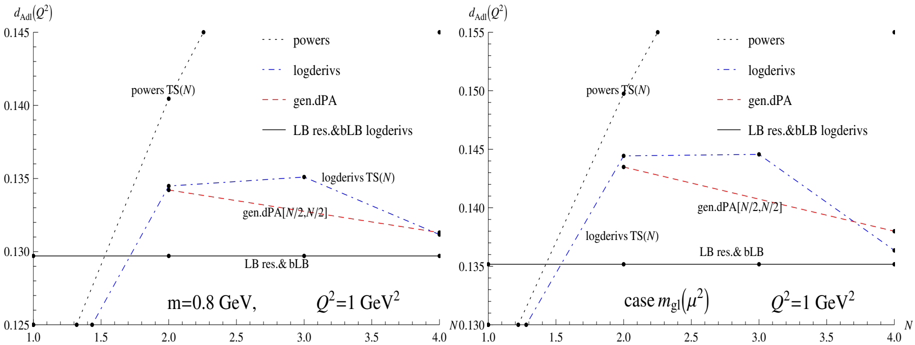

Figure: 15: The same as in Fig. 14, but for the two cases of effective gluon mass.

Numerical evidence (LB+bLB Adler function): convergence properties

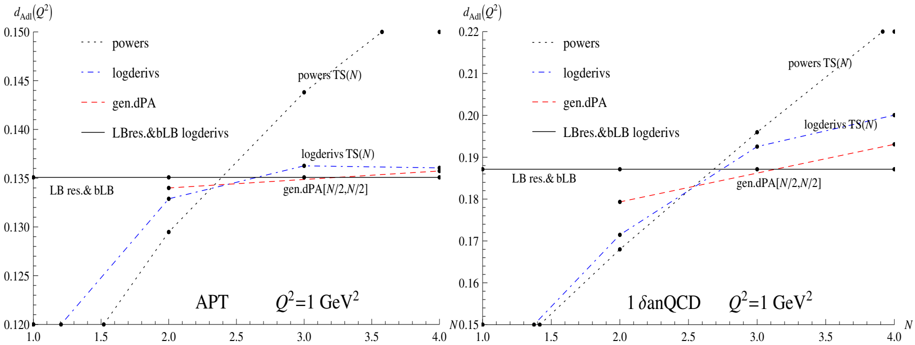

Figure: 16: The same as in Fig. 14, but for (F)APT and 1δanQCD model.

Numerical evidence (LB+bLB Adler function): convergence properties

Also in this (LB+beyondLB) case, we can see that in the IR fixed point frameworks the series in log derivatives behave significantly better than the corresponding power series; and that the generalized dPA method is often even better. These Figures include also the result of the LB resummation [i.e., the integral (56a)][2] with the three known beyond-LB terms added (here added in the form of log derivatives). This latter method is also considered as probably competitive with the generalized dPA method, at least at the considered order ($N = 4$).
On the other hand, in pQCD all methods are comparably bad.

[2] In the case of pQCD, the LB-integral has ambiguity due to the Landau singularities, and we took the Principal Value in this case.

Evaluation of timelike physical quantities in IR fixed point scenarios: massless case

Massless case

The described formalism is extended to timelike physical quantities $\mathcal{T}(s)$ ($s = -Q^2 > 0$), where we assume the existence of an integral transformation which relates $\mathcal{T}(s)$ with the corresponding spacelike quantity $\mathcal{F}(Q^2)$. The latter is evaluated as explained, for any complex Q^2, and the integral trasformation is applied on it to get $\mathcal{T}(s)$.

Often the integral transformation is the same as when $\mathcal{T}(s)$ is the ($e^+e^- \to \ \mathrm{hadrons}$) ratio $R(s)$ and $\mathcal{F}(Q^2)$ is the Adler function (log-derivative of the quark-current correlator)

$$\mathcal{F}(Q^2) = Q^2 \int_0^\infty \frac{d\sigma \ \mathcal{T}(\sigma)}{(\sigma + Q^2)^2} \ . \tag{69}$$

The inverse transformation is

$$\mathcal{T}(\sigma) = \frac{1}{2\pi i} \int_{-\sigma - i\varepsilon}^{-\sigma + i\varepsilon} \frac{d Q'^2}{Q'^2} \mathcal{F}(Q'^2) \ . \tag{70}$$

Evaluation of timelike physical quantities in IR fixed point scenarios: massless case

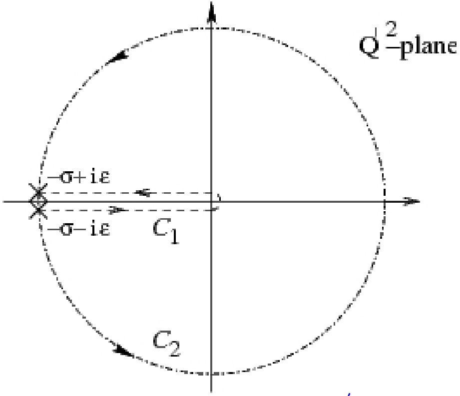

Figure: Possible paths $\mathcal{C}_1$ and $\mathcal{C}_2$ in the complex Q'^2-plane, for the integral (70).

Evaluation of timelike physical quantities in IR fixed point scenarios: massless case

Let us consider the case when the perturbation expansion of the spacelike quantity $\mathcal{F}(Q^2)$ in pQCD starts with $a(Q^2)^{\nu_0}$ (often: $\nu_0 = 1$; can be $\nu_0 > 1$, or noninteger)

$$\mathcal{F}(Q^2)_{\rm pt} = a(Q^2)^{\nu_0} + \mathcal{F}_1 a(Q^2)^{\nu_0+1} + \mathcal{F}_2 a(Q^2)^{\nu_0+2} + \cdots \ . \tag{71}$$

In IR fixed point scenarios this implies the following nonpower expansion, as explained in the previous Section:

$$\mathcal{F}(Q^2)_{\rm an} = \mathcal{A}_{\nu_0}(Q^2) + \mathcal{F}_1 \mathcal{A}_{\nu_0+1}(Q^2) + \mathcal{F}_2 \mathcal{A}_{\nu_0+2}(Q^2) + \cdots \ . \tag{72}$$

Evaluation of timelike physical quantities in IR fixed point scenarios: massless case

The application of the integral transformation (70) to this expression then gives the desired result. This can be performed term-by-term, leading to

$$\mathcal{T}(\sigma)_{\rm man} = \mathfrak{A}_{\nu_0}(\sigma) + \mathcal{F}_1 \mathfrak{A}_{\nu_0+1}(\sigma) + \mathcal{F}_2 \mathfrak{A}_{\nu_0+2}(\sigma) + \cdots \ , \qquad (73)$$

where the timelike (Minkowskian) couplings $\mathfrak{A}_{\nu}(\sigma)$ are defined as

$$\mathfrak{A}_{\nu}(\sigma) \equiv \frac{1}{2\pi i} \int_{-\sigma - i\varepsilon}^{-\sigma + i\varepsilon} \frac{dQ'^2}{Q'^2} \mathcal{A}_{\nu}(Q'^2) \ , \qquad (74)$$

and the inverse transformation is

$$\mathcal{A}_{\nu}(Q^2) = Q^2 \int_0^{\infty} \frac{d\sigma \ \mathfrak{A}_{\nu}(\sigma)}{(\sigma + Q^2)^2} \ . \qquad (75)$$

Evaluation of timelike physical quantities in IR fixed point scenarios: massless case

For example, to calculate the effective charge $\mathcal{T}(s) = r_{e^+e^-}(s)$ of the $(e^+e^- \to \text{ hadrons})$ ratio $R(s)$, we apply the mentioned evaluation to the effective charge $\mathcal{F}(Q'^2) = d(Q'^2)$ $(= \mathcal{A}(Q'^2) + \mathcal{O}(\mathcal{A}_2))$ of the Adler function $\mathcal{D}(Q'^2)$, for complex $Q'^2 = s\exp(i\phi)$, and integrate this expression in the contour integral (70).

Another example is the effective charge r_τ of the strangeless $V + A$ semihadronic τ decay ratio R_τ. After removing the effects of nonzero quark masses, this quantity can be expressed in terms of the effective charge of the Adler function $d_{\rm Adl}(Q^2)$, defined in Eqs. (54)-(55), as the following contour integral [Braaten, Narison, Pich (1988)]:

$$r_\tau = \frac{1}{2\pi} \int_{-\pi}^{+\pi} d\phi \; (1 + e^{i\phi})^3 (1 - e^{i\phi}) \; d_{\rm Adl}(Q^2 = {m_\tau}^2 e^{i\phi}) \; . \qquad (76)$$

Evaluation of timelike physical quantities in IR fixed point scenarios: massive case

Massive case; fractional powers

An example of a mass-dependent timelike observable which, in addition, involves noninteger (fractional) power analogs, is the partial decay width of the Higgs to $b\bar{b}$

$$\Gamma(H \to b\bar{b})(s) = \frac{N_c G_F}{4\pi\sqrt{2}} \sqrt{s}\ T(s) \ . \qquad (77)$$

Here, G_F is the Fermi constant, $s = {M_H}^2$ is the Higgs mass squared, and $T(s)$ is the imaginary part $\mathrm{Im}\Pi(-s - i\epsilon)/(6\pi s)$ of the correlator of the scalar current $J_b = m_b \bar{b} b$

$$\Pi(Q^2) = i(4\pi)^2 \int dx \exp(iq \cdot x) \langle 0 | T[J_b(x) J_b(0)] | 0 \rangle \ , \qquad (78)$$

($Q^2 = -q^2$), cf. Djouadi (Phys. Rept., 2008); Broadhurst, Kataev et al. (NPB, 2001; PoS A, 2008).

Evaluation of timelike physical quantities in IR fixed point scenarios: massive case

The timelike quantity $T(s)$ has the naive power expansion

$$T(s) = \overline{m}_b(s)^2 \left(1 + \sum_{n=1}^{\infty} t_n a(s)^n \right) , \tag{79}$$

where RS scale $\mu^2 = s$ was chosen. The corresponding spacelike quantity $F(Q^2)$ (a heavy scalar analog of the Adler function) is

$$F(Q^2) = Q^2 \int_0^{\infty} \frac{d\sigma \;\; T(\sigma)}{(\sigma + Q^2)^2} , \tag{80}$$

Evaluation of timelike physical quantities in IR fixed point scenarios: massive case

and its power expansion is

$$F(Q^2) = \overline{m}_b(Q^2)^2 \left(1 + \sum_{n=1}^{\infty} f_n a(Q^2)^n \right) \ , \tag{81}$$

The coefficients f_n in the expansion (81) were obtained by Chetyrkin (PLB, 1997) for $n = (1, 2, 3)$; and for $n = 4$ by Baikov, Chetyrkin and Kühn (PLB, 2006). When $N_f = 5$ (which applies here) they are:
$f_1 = 5.66667$; $f_2 = 42.032$; $f_3 = 353.229$; $f_4 = 3512.2$.
Relations between the (dimensionless) coefficients f_n and t_n are given by Chetyrkin, Kniehl and Sirlin (PLB, 1997).

Evaluation of timelike physical quantities in IR fixed point scenarios: massive case

Before evaluating $F(Q^2)$ in IR fixed point frameworks, and then $T(s)$ via the inverse integral transformation

$$T(\sigma) = \frac{1}{2\pi i} \int_{-\sigma - i\varepsilon}^{-\sigma + i\varepsilon} \frac{dQ'^2}{Q'^2} F(Q'^2) \ , \tag{82}$$

we must now first express $\overline{m}_b(Q^2)^2$ in terms of powers of $a(\mu^2)$ in pQCD. The RGE for the $\overline{\mathrm{MS}}$ running mass is

$$\frac{d\overline{m}(\mu^2)}{d \ln \mu^2} \equiv -\overline{m}(\mu^2)\ \gamma_m(a) = -\overline{m}(\mu^2) a \left(1 + \sum_{j \geq 1} \gamma_j a^j \right) \ , \tag{83}$$

where $a \equiv a(\mu^2)$; γ_j ($j = 1, 2, 3$) are known [Tarasov (NPB, 1981; JINR-Rep., 1982); Larin(PLB, 1993); Chetyrkin (PLB, 1997); Vermaseren et al. (PLB, 1997)]; γ_4 can be estimated, $\gamma_4 \approx 12$. [Kotikov, G.C. (JPG, 2012)].

Evaluation of timelike physical quantities in IR fixed point scenarios: massive case

Integration of the RGE (83) and the RGE for $a(\mu^2)$, Eq. (14), then gives

$$\overline{m}_b{}^2(\mu^2) = \hat{m}_b{}^2 \; a(\mu^2)^{\nu_0} \left(1 + \sum_{j \geq 1} \mathcal{M}_j a(\mu^2)^j \right) \tag{84}$$

where $\hat{m}_b{}^2$ is a renormalization scale invariant mass, $\nu_0 = 2/\beta_0 = 1.04348$. The coefficients $\mathcal{M}_j$ ($j = 1, 2, 3, 4$) are functions of β_0, $c_k \equiv \beta_k/\beta_0$ and γ_k ($k \leq j$), i.e., they are known. For the case here ($N_f = 5$) they are:
$\mathcal{M}_1 = 2.35098$; $\mathcal{M}_2 = 4.38319$; $\mathcal{M}_3 = 3.87308$; $\mathcal{M}_4 = -22.2155$.
The invariant mass $\hat{m}_b$ can be determined from the $\overline{\mathrm{MS}}$ mass
$\overline{m}_b(\overline{m}_b{}^2) = 4.232$ GeV, and is:
$\hat{m}_b = 15.33$ GeV.

Evaluation of timelike physical quantities in IR fixed point scenarios: massive case

The dimensionless analogs of the spacelike $F(Q^2)$ and timelike $T(s)$ can be defined now: $\mathcal{F}(Q^2) \equiv F(Q^2)/\hat{m}_b{}^2$ and $\mathcal{T}(s) \equiv T(s)/\hat{m}_b{}^2$. Applying the analytization $a^{\nu_0+n} \mapsto \mathcal{A}_{\nu_0+n}$ in the IR fixed point scenarios, this gives

$$\begin{aligned} \mathcal{F}(Q^2) \equiv \frac{1}{\hat{m}_b{}^2} F(Q^2) &= a(Q^2)^{\nu_0} + \sum_{n \geq 1} \mathcal{F}_n a(Q^2)^{\nu_0+n} \\ &\mapsto \mathcal{A}_{\nu_0}(Q^2) + \sum_{n \geq 1} \mathcal{F}_n \mathcal{A}_{\nu_0+n}(Q^2) , \end{aligned} \tag{85}$$

for any complex Q^2, where the coefficients $\mathcal{F}_n$ are now combinations of the coefficients f_j (of F) and $\mathcal{M}_k$ (of $\overline{m}_b(Q^2)$)

$$\mathcal{F}_n = f_n + f_{n-1}\mathcal{M}_1 + \cdots f_1 \mathcal{M}_{n-1} + \mathcal{M}_n \ . \tag{86}$$

Evaluation of timelike physical quantities in IR fixed point scenarios: massive case

The timelike dimensionless quantity $\mathcal{T}(s)$ (with $s = {M_H}^2$)

$$\mathcal{T}(s) \equiv \frac{T(s)}{{\hat{m}_b}^2} = \frac{\Gamma(H \to b\bar{b})(s)}{{\hat{m}_b}^2 N_c G_F \sqrt{s}/(4\pi\sqrt{2})} \ , \qquad (87)$$

and thus the partial decay width $\Gamma(H \to b\bar{b})$, are obtained in such scenarios by applying to the (truncated) nonpower series (85) the integral transformation (70).

In fractional APT (FAPT) [Bakulev, Mikhailov and Stefanis (BMS)], this quantity was calculated by BMS (PRD, 2007). In other (analytic) models which are closer to pQCD at high energies, this quantity was evaluated by Kotikov and G.C. (JPG, 2012). It turns out that the result of the described method for $\Gamma(H \to b\bar{b})$ is the same in pQCD and in any such IR fixed point scenarios where $\rho(\sigma) = \rho^{(\mathrm{pt})}(\sigma)$ at $\sigma \geq {M_H}^2$. These results are given in Fig. 18.

Evaluation of timelike physical quantities in IR fixed point scenarios: massive case

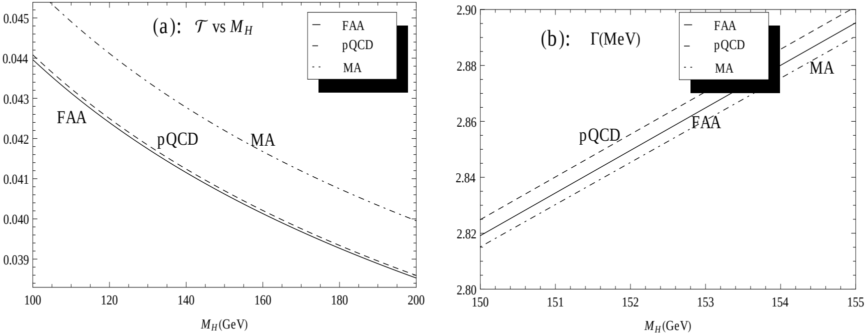

Figure: (a) The (dimensionless) $\mathcal{T}(s)$, as defined in equation (87), as a function of the Higgs mass $M_H = \sqrt{s}$: for our approach ("fractional analytic" – FAA) of Eqs. (70),(85), 87); for the usual pQCD approach of equation (79) (in both cases $\overline{\Lambda} = 0.213$ GeV at $N_f = 5$); and for the APT/MA model with FAA approach ($\overline{\Lambda}_{\rm APT} = 0.260$ GeV at $N_f = 5$); (b) the same but now for the decay width $\Gamma(H \to b\bar{b})$.

Summary

- Lattice calculations and calculations using DSE and/or BSE indicate that the QCD coupling $\mathcal{A}(Q^2)$ freezes to a finite value $\mathcal{A}(0)$ (IR FP).
- We considered the IR FP frameworks: with effective gluon mass; (F)APT; 1δanQCD. And compared them with pQCD.
- We argued that power expansions should not be used, but rather the log derivative expansions and a resummation based on them (generalized dPA), because then: the NP contributions are correctly accounted for, the RScl dependence is in general weaker, and the convergence properties improve.
- We numerically showed how this works in practice, by evaluations of $d_{\rm Adl}(Q^2)$ (LB, and LB+bLB).
- Extension of the formalism to the timelike quantities.

Only part of NP can be incorporated in a universal IRFP $\mathcal{A}(Q^2)$; higher-twist OPE terms should be added to account for other NP contributions. Therefore, IRFP scenarios should fulfill at $|Q^2| > \Lambda^2$: $\mathcal{A}(Q^2) - a(Q^2) \sim (\Lambda^2/Q^2)^N$ with a large N (e.g., $N \geq 3, 4, 5$).